Analysis of fly-around mission with spinning tether system for space station observation

Yang Hang

2024.6.2

CONTENTS

Introduction

Methods

Results

Future work

PART 1

Introduction

Small fly-around satellites?

Nanosatellites are equipped with monitoring devices to perform a periodical surrounding relative to the space station [1-2].

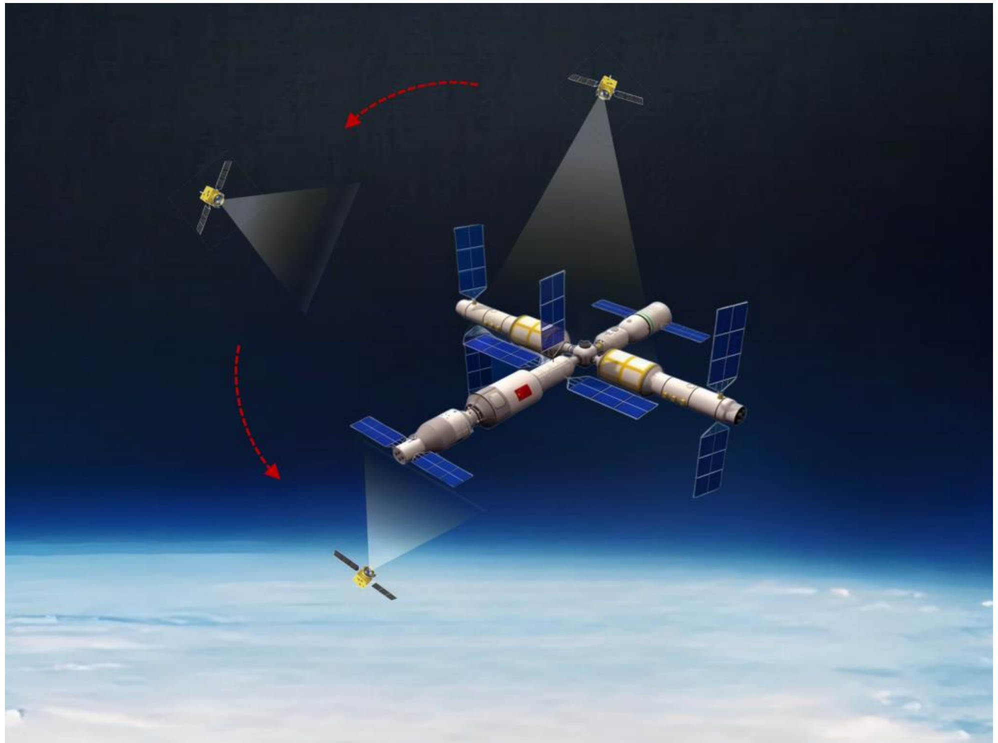

Limitation

Fast controlled fly-around

reling on impulsive thrust, leading to high fuel consumption and an inability to sustain long-term monitoring[16,17].

Natural fly-around.

complex orbit changes and gradual approach control, prolonged period of natural fly-around mode[6,11].

Fly-around mission process with STS

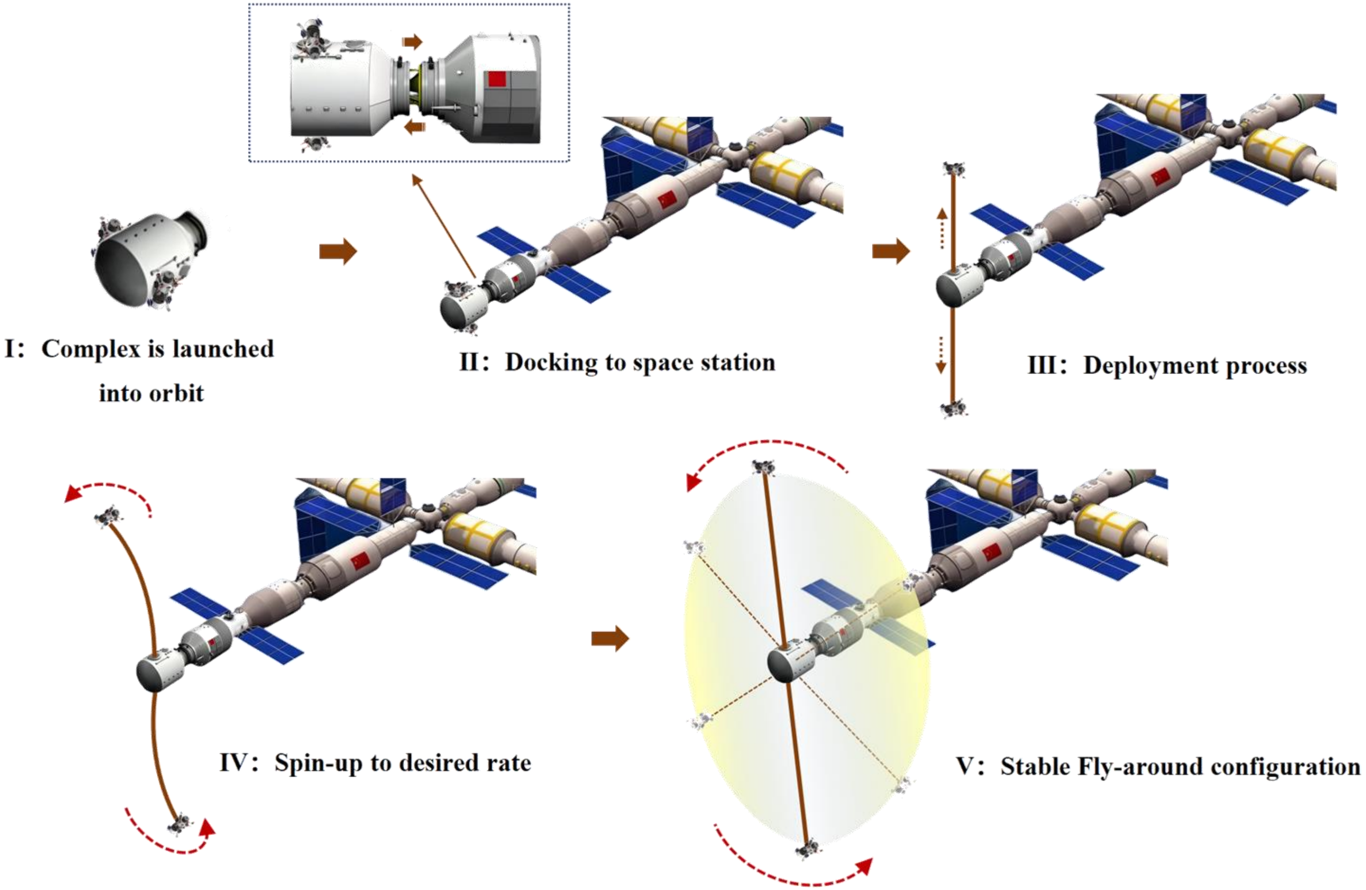

I. A tethered satellites system in undeployed state is launched into orbit

II. docking with the space station module.

III. The satellites are deployed to designated positions around the space station,

IV. STS starts spin up to desired spinning rate

V. Form a stable fly-around configuration.

Two different fly-around schemes

During the whole fly-around process, **maintaining a stable spinning configuration** in these planes is crucial for the tether system to effectively prevent entanglement with space station's solar panels.

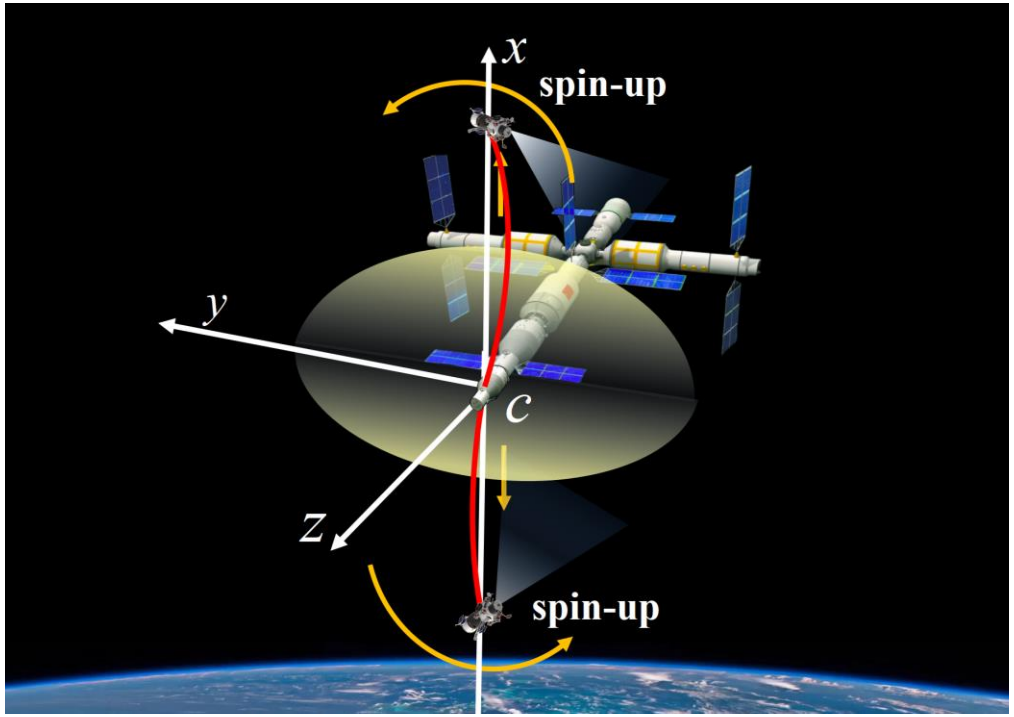

(a) Planar fly-around

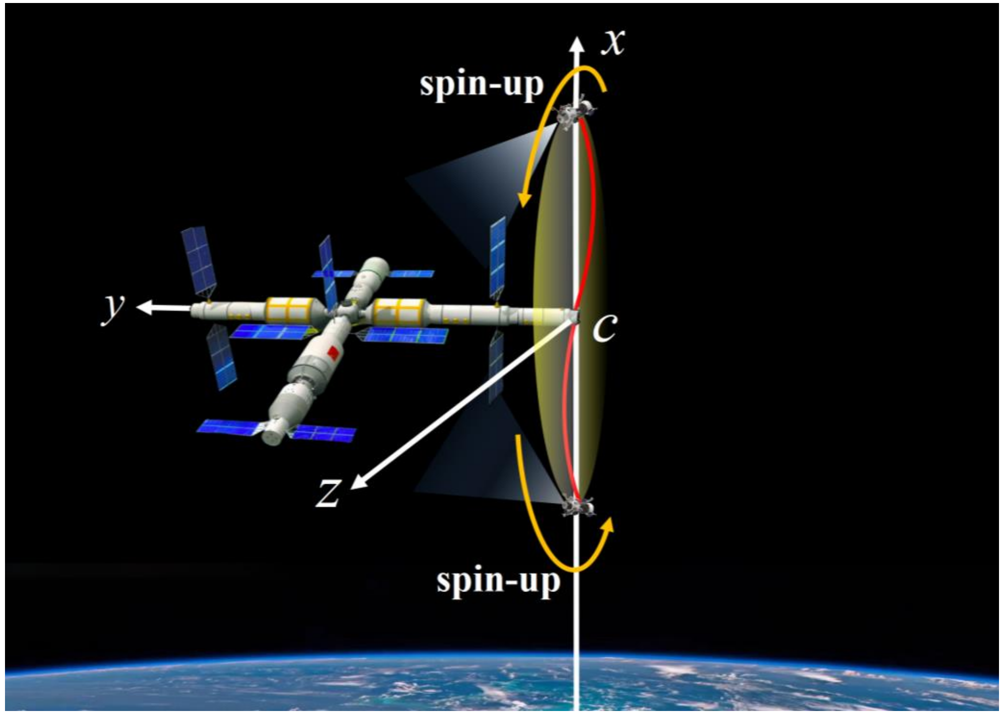

(b) Vertical fly-around

PART 2

Methods

Dynamic model

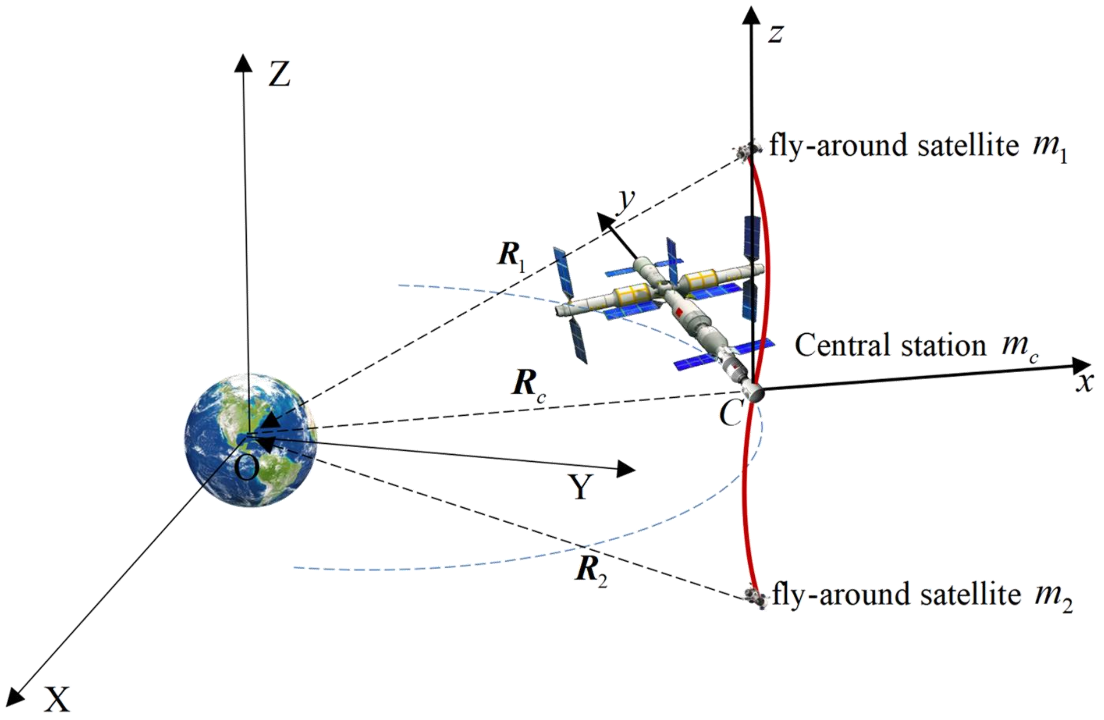

$$m_i \frac{d^2 \boldsymbol{R}_i}{dt^2} = \boldsymbol{G}_i + \boldsymbol{D}_i + \boldsymbol{T}_i + \boldsymbol{F}_i, \ i = 1, 2 \tag{1}$$

$$L = |\Delta \boldsymbol{R}|, \sin\theta = \frac{\Delta y}{\sqrt{\Delta x^2 + \Delta y^2}}, \sin\beta = \frac{\Delta z}{|\Delta \boldsymbol{R}|} \tag{2}$$

I. The lumped model avoids the problem of singularities.

II. When TFSF is spinning spatially, the coupling definition of two angles leads to incorrect calculation of angles, which makes it difficult to study STS spinning motion.

A new spinning coordinate system

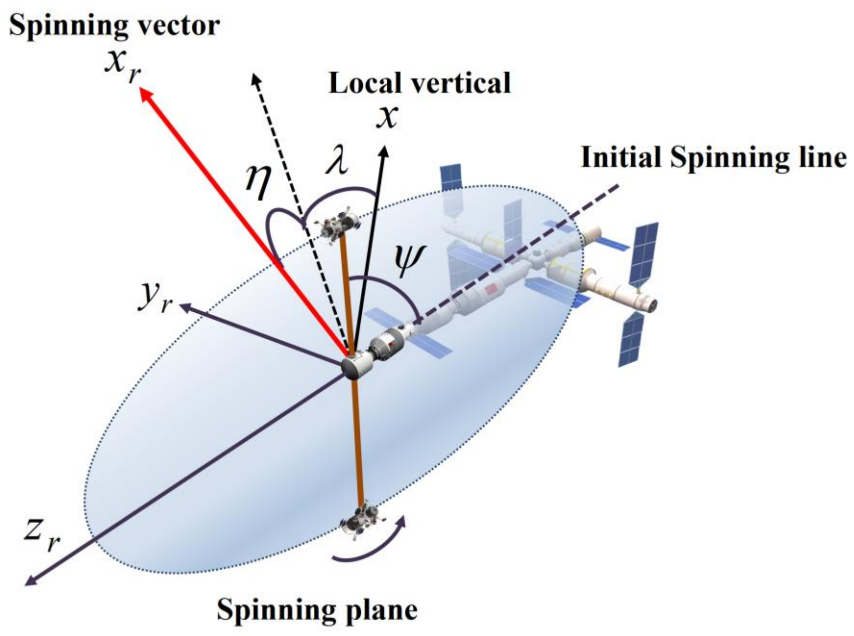

The transition matrix from the orbital motion coordinate system to the spinning plane coordinate system is represented as

$$\boldsymbol{L}_{cs} = \boldsymbol{L}_{\psi}\boldsymbol{L}_{\eta}\boldsymbol{L}_{\lambda} \tag{1}$$

where

$$\boldsymbol{L}_{\psi} = \begin{bmatrix} 1 & 0 & 0 \\ 0 & \cos\psi & -\sin\psi \\ 0 & \sin\psi & \cos\psi \end{bmatrix}, \boldsymbol{L}_{\eta} = \begin{bmatrix} \cos\eta & 0 & -\sin\eta \\ 0 & 1 & 0 \\ \sin\eta & 0 & \cos\eta \end{bmatrix}, \boldsymbol{L}_{\lambda} = \begin{bmatrix} \cos\lambda & \sin\lambda & 0 \\ -\sin\lambda & \cos\lambda & 0 \\ 0 & 0 & 1 \end{bmatrix}$$

the positions and velocity of fly-around satellites in $Cx_r y_r z_r$ are :

$$\begin{cases} \boldsymbol{P}_1 = \begin{bmatrix} 0 & L_b \sin\psi_b & -L_b \cos\psi_b \end{bmatrix}^T \\ \boldsymbol{P}_2 = \begin{bmatrix} 0 & -L_b \sin\psi_b & L_b \cos\psi_b \end{bmatrix}^T \\ \boldsymbol{V}_1 = \begin{bmatrix} 0 & \dot{\psi}_b L_b \cos\psi_b & \dot{\psi}_b L_b \sin\psi_b \end{bmatrix}^T \\ \boldsymbol{V}_2 = \begin{bmatrix} 0 & -\dot{\psi}_b L_b \cos\psi_b & -\dot{\psi}_b L_b \sin\psi_b \end{bmatrix}^T \end{cases} \tag{2}$$

Reference trajectories transition from $Cx_r y_r z_r$ to $OXYZ$

The spinning motion in the orbital motion coordinate system is calculated as follows:

$$\boldsymbol{P}_i^{Cxyz} = \boldsymbol{L}_{cs}^{-1}\boldsymbol{P}_i, \boldsymbol{U}_i^{Cxyz} = \boldsymbol{L}_{cs}^{-1}\boldsymbol{V}_i, i = 1,2. \quad (3)$$

The spinning velocity of the fly-around satellites in the orbital motion coordinate system is calculated as:

$$\boldsymbol{V}_i^{Cxyz} = \boldsymbol{U}_i^{Cxyz} + \boldsymbol{V}_q^{Cxyz} \quad (4)$$

where $\boldsymbol{V}_q^{Cxyz} = \boldsymbol{V}_c^{Cxyz} + \boldsymbol{V}_{ei}^{Cxyz} + \boldsymbol{V}_{rei}^{Cxyz}, \boldsymbol{V}_c^{Cxyz} = \begin{bmatrix} 0 & r_c\omega_c & 0 \end{bmatrix}^T, \boldsymbol{V}_{ei}^{Cxyz} = \boldsymbol{\omega}_{ci}^{Cxyz} \times \boldsymbol{P}_i^{Cxyz}, \boldsymbol{V}_{rei}^{Cxyz} = \boldsymbol{\omega}_{ri}^{Cxyz} \times \boldsymbol{P}_i^{Cxyz}$

$\boldsymbol{\omega}_{ci}^{Cxyz} = [0 \quad 0 \quad \omega_c]^T, \boldsymbol{\omega}_{ri}^{Cxyz} = L_{cs}{}^T[0 \quad \dot{\eta} \quad 0]^T + L_\lambda{}^T[0 \quad \dot{\lambda} \quad 0]^T$

the positions and velocities of the two fly-around satellites in the inertial system $OXYZ$ are calculated as :

$$\begin{aligned} \boldsymbol{R}_i &= \boldsymbol{L}_{co}\boldsymbol{P}_i^{Cxyz} + \boldsymbol{L}_{co}\boldsymbol{R}_c \\ \boldsymbol{V}_i &= \boldsymbol{L}_{co}\boldsymbol{V}_i^{Cxyz} \end{aligned} \quad (5)$$

where $\boldsymbol{R}_c = [r_c \quad 0 \quad 0]^T$

NORTHWESTERN POLYTECHNICAL UNIVERSITY

Reference trajectories transition from $Cx_r y_r z_r$ to $OXYZ$

The spinning plane vector is $\boldsymbol{n}_r = \begin{bmatrix} n_x & n_y & n_z \end{bmatrix}^T$, $\Delta \boldsymbol{P}_i^{Cx_r y_r z_r} = \begin{bmatrix} x_{\Delta P_i} & y_{\Delta P_i} & z_{\Delta P_i} \end{bmatrix}^T$ is the absolute vector difference between fly-around satellites in the $Cx_r y_r z_r$ frame

η and λ can be solved as follows:

$$\eta = -\arcsin\left(\frac{n_z}{\sqrt{n_x^2 + n_y^2 + n_z^2}}\right), \lambda = \begin{cases} \dfrac{\pi}{2} & n_x = 0, n_y = 0 \\ \arcsin\left(\dfrac{n_y}{\sqrt{n_x^2 + n_y^2}}\right) & \text{otherwise} \end{cases} \quad (6)$$

$$\psi_b = \begin{cases} -\arcsin\left(\dfrac{y_{\Delta P_i}}{\sqrt{y_{\Delta P_i}^2 + z_{\Delta P_i}^2}}\right) + \pi & (z_{\Delta P_i} > 0) \\ \arcsin\left(\dfrac{y_{\Delta P_i}}{\sqrt{y_{\Delta P_i}^2 + z_{\Delta P_i}^2}}\right) & (z_{\Delta P_i} \le 0, y_{\Delta P i} \ge 0) \\ \arcsin\left(\dfrac{y_{\Delta P_i}}{\sqrt{y_{\Delta P_i}^2 + z_{\Delta P_i}^2}}\right) + 2\pi & (z_{\Delta P_i} \le 0, y_{\Delta P i} < 0) \end{cases} \quad (7)$$

Controller design

Dynamic eqution of STS can be rewritten as

$$\begin{aligned} \dot{\xi}_1 &= \xi_2 \\ \dot{\xi}_2 &= \boldsymbol{f}(\xi) + \boldsymbol{g}(\xi)\boldsymbol{u} \end{aligned} \tag{1}$$

where $\xi = [\boldsymbol{R}, \boldsymbol{v}]^T$, $\boldsymbol{f}(\xi) = \frac{1}{\boldsymbol{m}}(\boldsymbol{G}+\boldsymbol{D}+\boldsymbol{T})$, $\boldsymbol{g}(\xi) = \frac{1}{\boldsymbol{m}}$

The error function is defined as follows

$$\tilde{\xi} = \xi - \xi_d \tag{2}$$

where $\xi_d = [\boldsymbol{R}_d, \boldsymbol{v}_d]^T$ is reference trajectory. The tracking error dynamics is expressed as

$$\begin{aligned} \tilde{\xi}_1 &= \xi_1 - \xi_{d1} \\ \tilde{\xi}_2 &= \xi_2 - \boldsymbol{\alpha} \end{aligned} \tag{3}$$

where $\tilde{\xi}_1$, $\tilde{\xi}_2$ are respectively the error of position and velocity, $\boldsymbol{\alpha} = -k_a \tilde{\xi}_1 + \dot{\xi}_{d1}$ is virtual controls, k_a is the control coefficient

The control law is defined as

$$\boldsymbol{u} = -\boldsymbol{f}(\xi) + \boldsymbol{m}\dot{\boldsymbol{\alpha}} - \boldsymbol{m}k_b\dot{\tilde{\xi}}_2 \tag{4}$$

Controller design

A positive definite Lyapunov function is defined as

$$\boldsymbol{V} = \frac{1}{2}\tilde{\xi}_1^T\tilde{\xi}_1 + \frac{1}{2}\tilde{\xi}_2^T\tilde{\xi}_2 \quad (5)$$

The derivative of the Lyapunov function is

$$\begin{aligned}\dot{\boldsymbol{V}} &= \tilde{\xi}_1^T\dot{\tilde{\xi}}_1 + \tilde{\xi}_2^T\dot{\tilde{\xi}}_2 \\ &= \tilde{\xi}_1^T(\xi_2 - \dot{\tilde{\xi}}_{d1}) - k_b\tilde{\xi}_2^T\tilde{\xi}_2 \\ &= \tilde{\xi}_1^T(-k_a\tilde{\xi}_1 + \tilde{\xi}_2) - k_b\tilde{\xi}_2^T\tilde{\xi}_2 \\ &\le \left(\frac{1}{2} - k_a\right)\tilde{\xi}_1^T\tilde{\xi}_1 + \left(\frac{1}{2} - k_b\right)\tilde{\xi}_2^T\tilde{\xi}_2\end{aligned} \quad (6)$$

when the control coefficients k_a and k_b are both greater than 1/2, $\dot{\boldsymbol{V}} < 0$. the law in (4) ensures asymptotic stability of system.

PART 3

Results

Planar fly-around

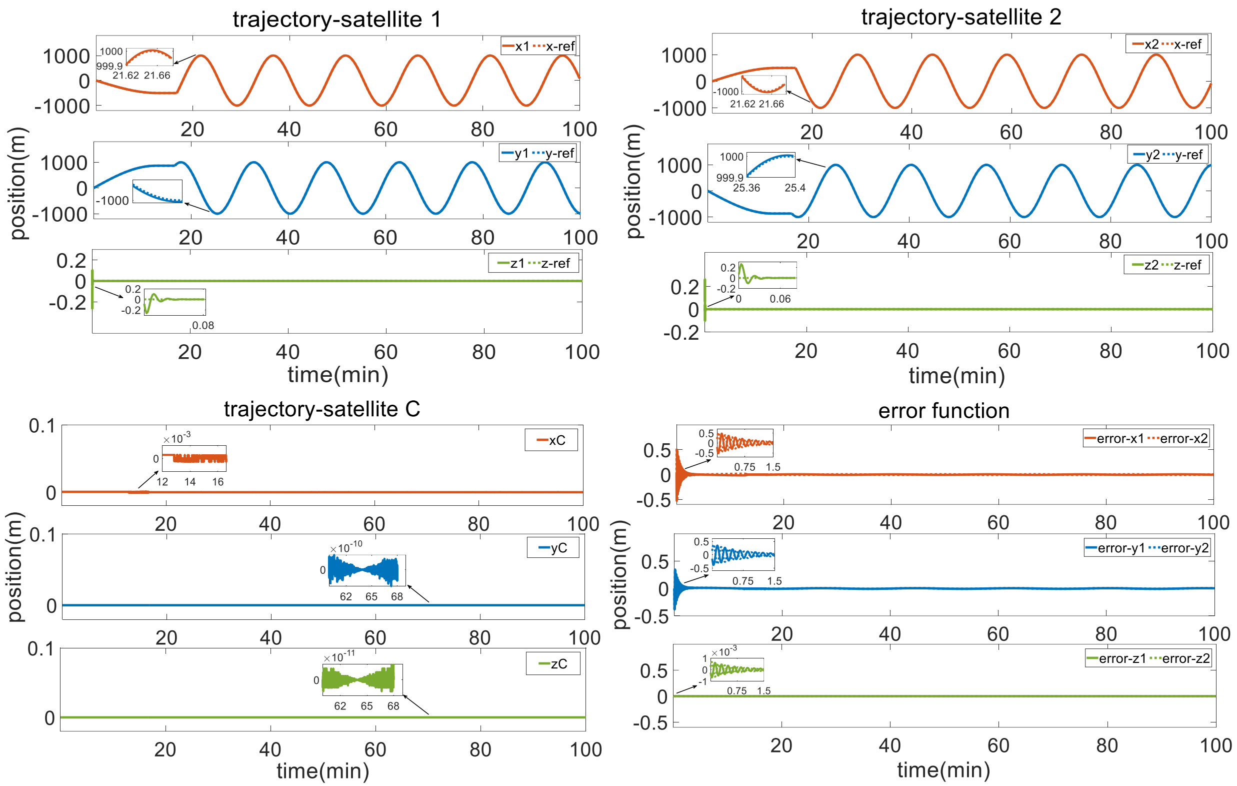

Fig. 1. Trajectories of satellites motion

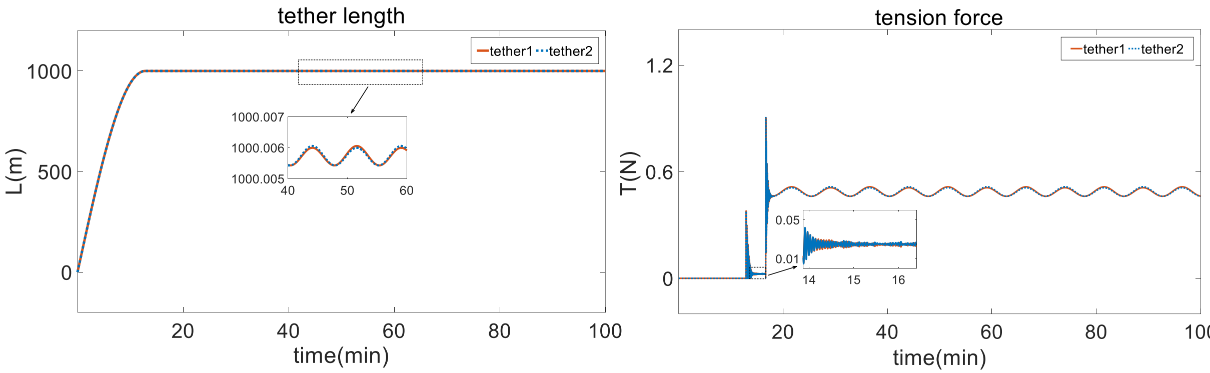

Fig. 2. Main characteristics of tether length and tension

Planar fly-around

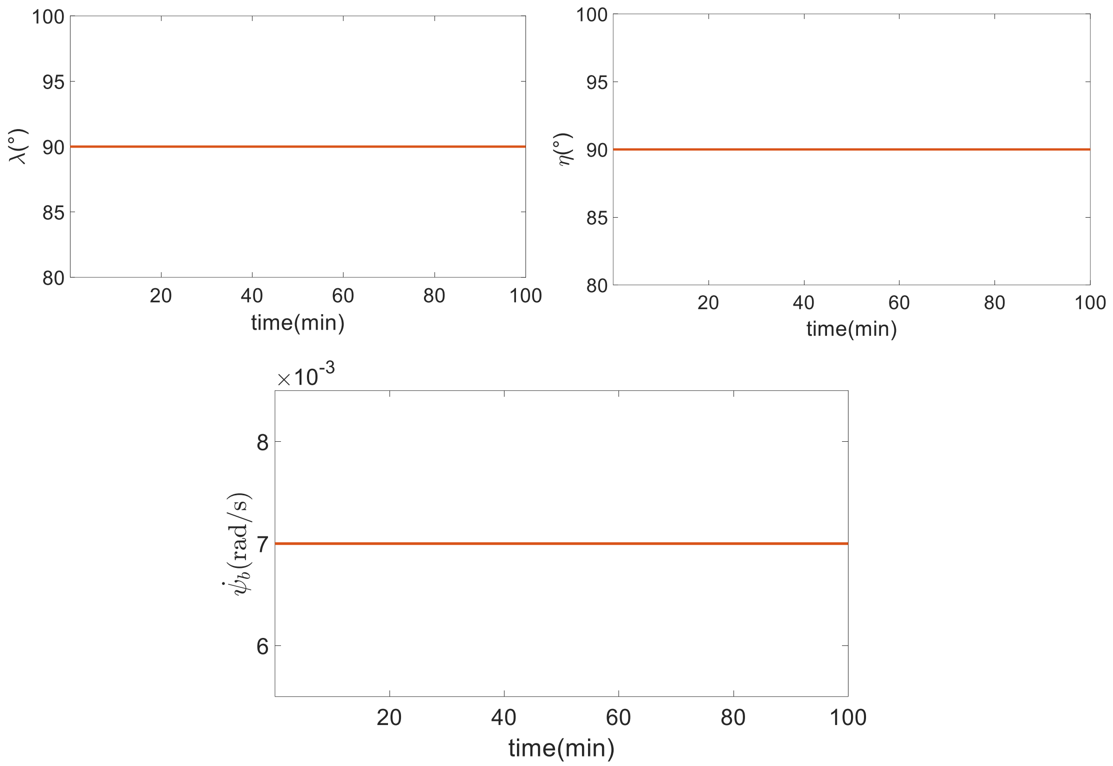

Fig. 1. variations in the angle λ, η and ψ_b

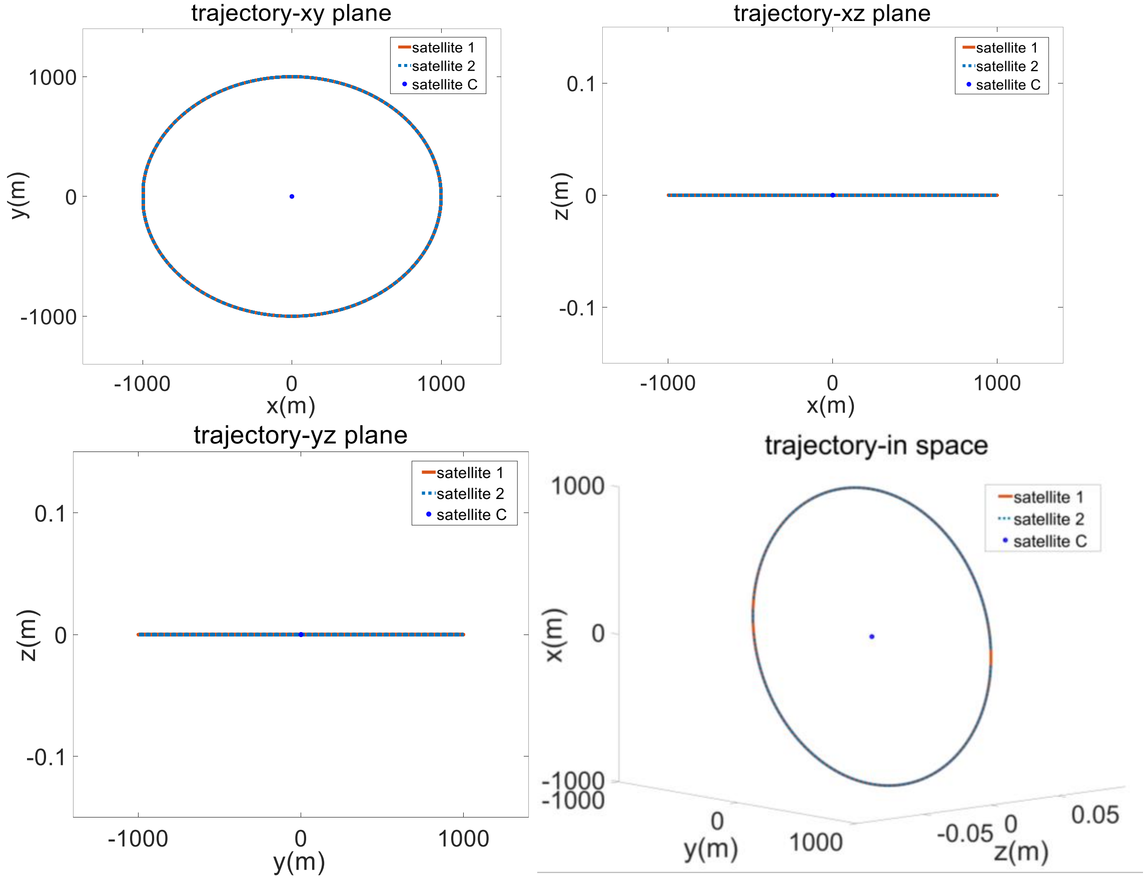

Fig. 2. Trajectories of fly-around satellites during the planar fly-around process

Results

西北工業大學 NORTHWESTERN POLYTECHNICAL UNIVERSITY

Vertical fly-around

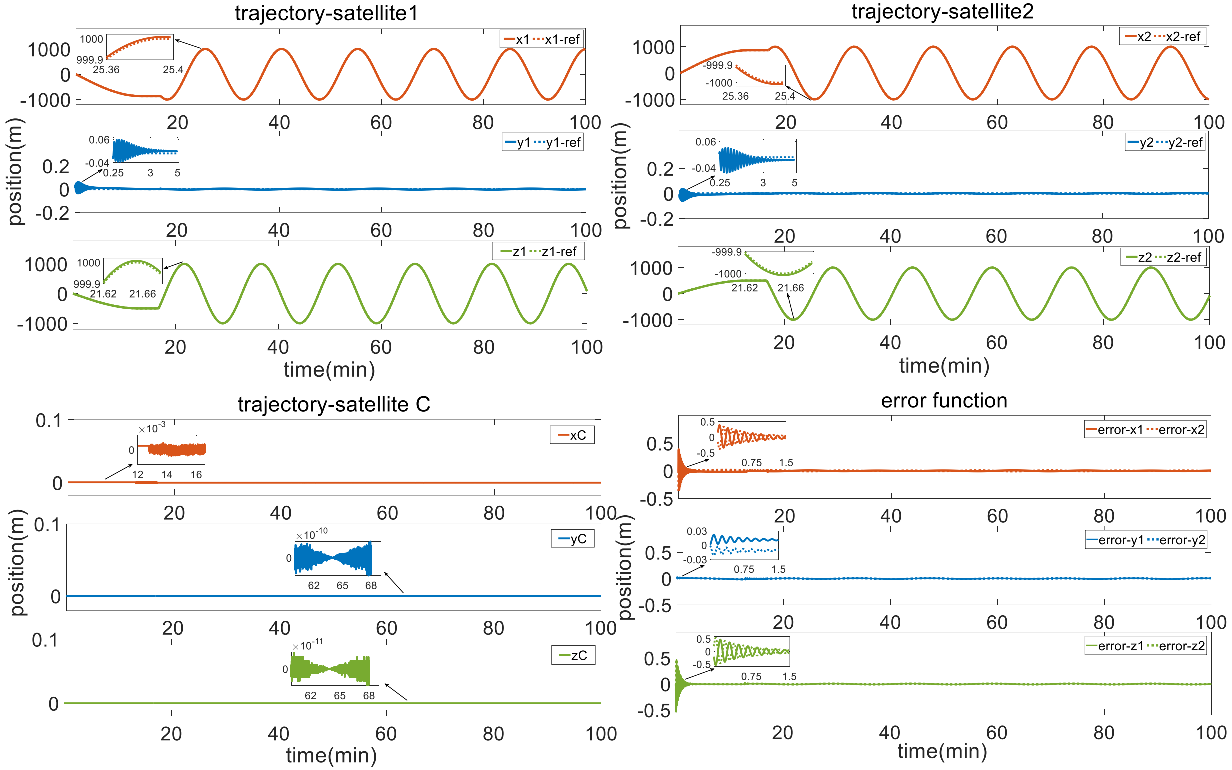

Fig. 1. Trajectories of satellites motion

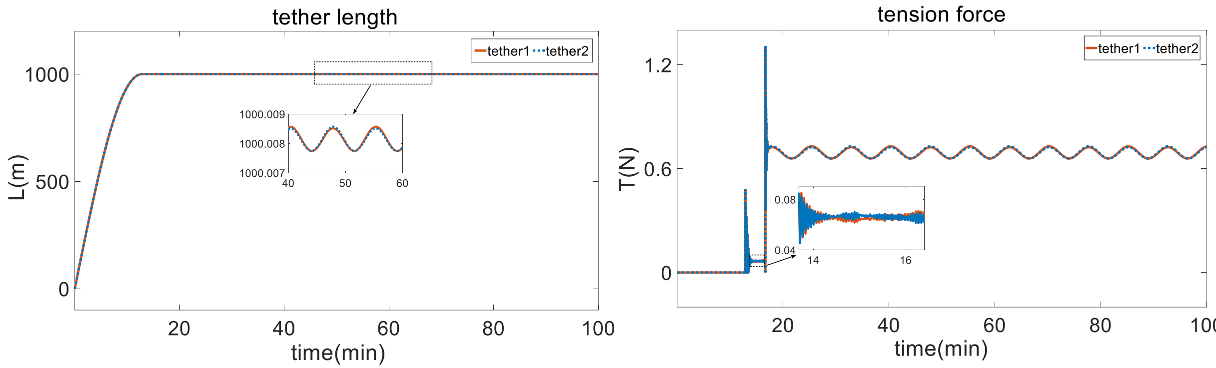

Fig. 2. Main characteristics of tether length and tension

西北工业大学 NORTHWESTERN POLYTECHNICAL UNIVERSITY

Vertical fly-around

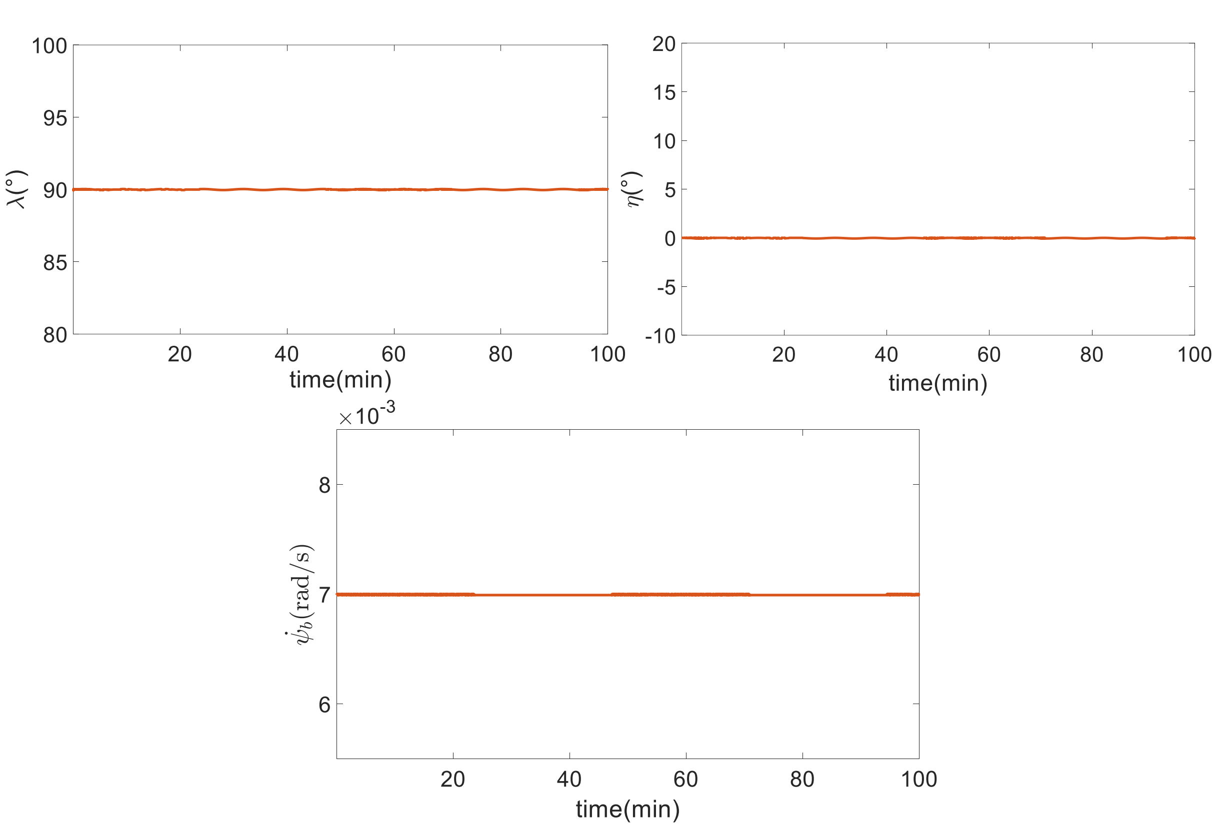

Fig. 1. variations in the angle λ, η and ψ_b

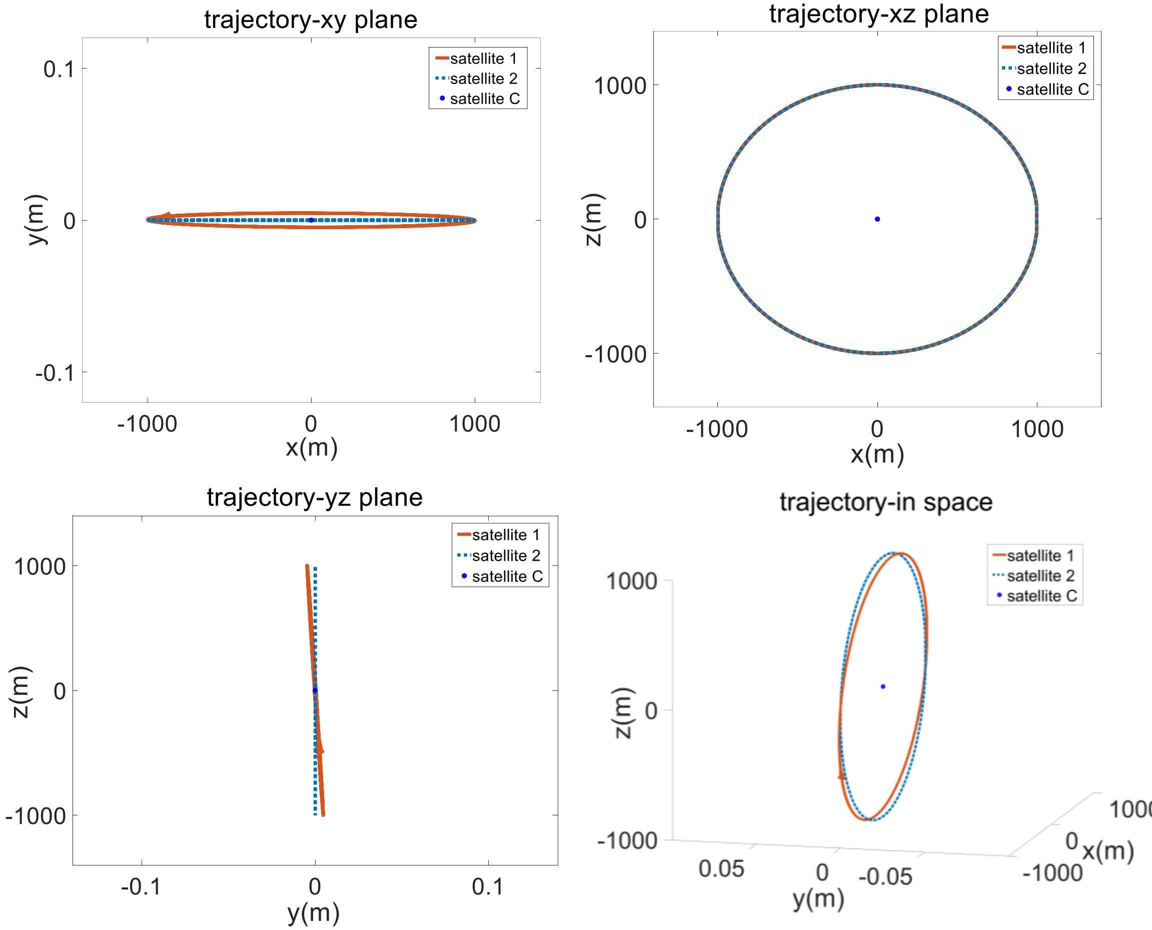

Fig. 2. Trajectories of fly-around satellites during the vertical fly-around process

Fuel consumption analysis

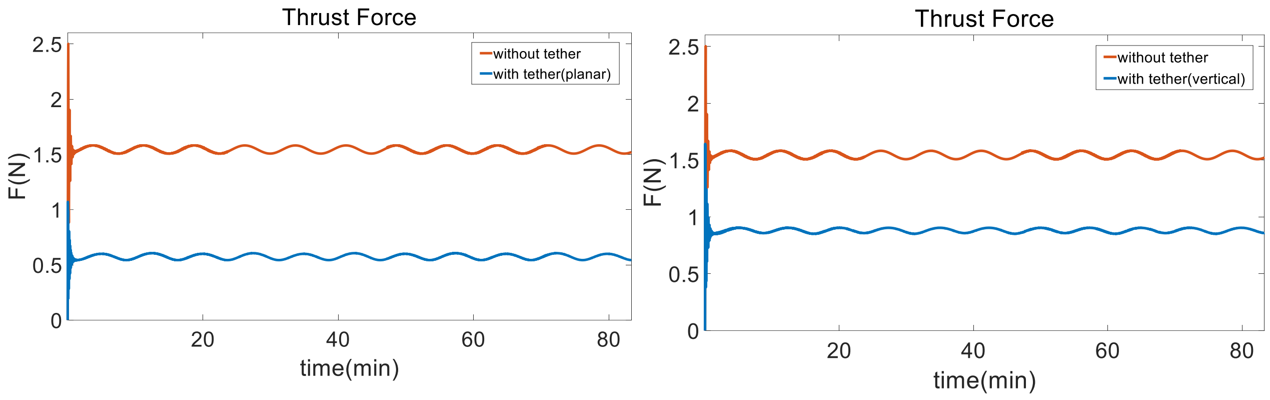

Fig. 1. comparison of thrust with/without tether

Table 1 Comparison of impulse with/without tether within 1 orbital period

	Non-tethered fly-around	Tethered fly-around
Scheme I (Planar)	Impulse consumption (16673.8 N.s)	Impulse consumption (6196.6 N.s)
Scheme II (Vertical)	Impulse consumption (16673.8 N.s)	Impulse consumption (9504.2 N.s)

During planar spin, 62.8% saving of impulse can be achieved compared to the traditional untethered fly-around, while the vertical fly-around scheme results in 42.9% decrease in impulse.

Conclusion

1. This study proposes a novel STS fly-around scheme to conduct space stations fly-around mission and validates its feasibility.

2. The STS is modeled based on Newton-Euler method with a novel description of spinning motion, to overcome the singularity and coupling issues of commonly used models.

3. Considering the structural constraints of the space station, the study designs two spinning fly-around schemes and reference fly-around trajectories. Additionally, a backstepping controller is proposed for the tracking of fly-around satellites motion, ensuring s atable fly-around configuration during the whole spinning process.

4. Comparisons of fuel consumption among different fly-around schemes within one orbital period demonstrate that the STS fly-around scheme significantly reduces energy consumption compared to the untethered fly-around scheme.
During planar spin, 62.8% saving of impulse can be achieved compared to the traditional untethered fly-around, while the vertical fly-around scheme results in 42.9% decrease in impulse.

References

[1] F. Wang, L. Zhang, Y. Xu, K Wang, Z. Qiao, D. Guo, J. Wang, Development of the on-orbit maintenance and manipulation workbench (MMW) for the Chinese space station, Acta Astronautica. 214 (2024) 366-379.

[2] C. Sun, Y. SUN, X. Yu, Q. Fang, Rapid Detection and Orbital Parameters' Determination for Fast-Approaching Non-Cooperative Target to the Space Station Based on Fly-around Nano-Satellite, Remote Sensing. 15 (2023) 1213.

[3] H. Zhou, Z. Dang, Y. Zhang, J. Yuan, Collision-free control of a nano satellite in the vicinity of China Space Station using Lorentz augmented composite artificial potential field, Acta Astronautica. 203 (2023) 88-102.

[4] P. M. Trivailo, F. Wang, H. Zhang, Optimal attitude control of an accompanying satellite rotating around the space station, Acta Astronautica. 64 (2009) 89-94.

[5] J. Guo, K. Ma, Y. Yao, Orbit and control design for forming and keeping fly-around, In: 2009 Chinese Control and Decision Conference (CCDC), 2009, pp. 729-734.

[6] S. Bai, C. Han, Y. Rao, X. Sun, Y. Sun, New fly-around formations for an elliptical reference orbit, Acta Astronautica. 171 (2020) 335-351.

[7] T.M. Davis, D. Melanson, XSS-10 microsatellite flight demonstration program results, In: Spacecraft platforms and infrastructure (SPIE), 2004, pp. 16-25.

[8] D. Li, Z. Zhu, R. Zhang, H. Cheng, J. Zhang, S. Wan, The Design and In-Orbit Test of the Companion Microsatellite Attitude Control System in SZ-7 Flight Mission, Journal of Astronautics. 32 (2011) 495-501.

[9] J. Hu, H. Su, W. Wu, J. Chu, The stable orbit of the small satellite flying around the space station and the orbit maintenance, in: Proceedings of the 39th IEEE Conference on Decision and Control, 2000, pp. 4181-4186.

[10] Y. Masutani, M. Matsushita, F. Miyazaki, Fly around maneuvers on a satellite orbit by impulsive thrust control, In: 2001 IEEE International Conference on Robotics & Automation (ICRA), 2006, pp. 421-426.

References

[11] Y. Chang, Y. Chen, Y. Xian, D. Zhang, J. Gao, Configuration design maintenance of fly-around trajectory for target monitoring in elliptical orbit, Systems Engineering and Electronics. 39 (2017) 1317-1324.

[12] J. Luo, W. Zhou, J. Yuan, A General Method of Trajectory Design and Guidance for Fast Satellite Circumnavigation, Journal of Astronautics. 28 (2007) 628-632.

[13] Y. Qi, Y. Jia, Forming and Keeping Fast Fly-Around Under Constant Thrust, Advances in Space Research. 48 (2011) 1421-1431.

[14] G. Wang, W. Zheng, Y. Meng, G. Tang, Fast Fly Around Formation Design Based on Continuous Low Thrust, in: 2010 3rd International Symposium on Systems and Control in Aeronautics and Astronautics (ISSCAA), 2010, pp. 1095-1100.

[15] Q. Hu, J. Xie, X. Liu, Trajectory optimization for accompanying satellite obstacle avoidance, Aerospace Science and Technology. 82 (2018) 220-233.

[16] R. Zhang, C. Han, Y. Rao, J. Yin, Spacecraft fast fly-around formations design using the bi-teardrop configuration, J. Guidance. Control Dynamics. 41 (2018) 1542-1555.

[17] Z. Lin, B. Wu, D. Wang, Specific tracking control of rotating target spacecraft under safe motion constraints, IEEE Trans. Aerospace Electronic Systems, 59 (2023) 2422-2438.

[18] M. Van Pelt., Space Tethers and Space Elevators, Springer Science &Business Media, New York, 2009, pp. 20–22, 23–27.

[19] M. Shan, L. Shi, Post-capture control of a tumbling space debris via tether tension, Acta Astronautica. 180 (2021) 317-327.

[20] P. Huang, F. Zhang, L. Chen, Z. Meng, Y. Zhang, Z. Liu, Y. Hu, A review of space tether in new applications, Nonlinear Dynamics. 94(1) (2018) 1-19.

References

[21] M. Zheng, Y. Zhang, L. Fan, Y. Xu, Retrieval dynamics and control for approach of tethered on-orbit service satellite, Advances in Space Research. 71(12) (2023) 4995-5006.

[22] M. L. Cosmo, E. C. Lorenzini, Tethers in Space Handbook, 3rded., NASA, 1997.

[23] A. Li, H. Tian, C. Wang. Fixed-time terminal sliding mode control of spinning tether system for artificial gravity environment in high eccentricity orbit, Acta Astronautica. 177 (2020) 834-841.

[24] X. Gou, A. Li, H. Tian, C. Wang, H. Lu, Overload control of artificial gravity facility using spinning tether system for high eccentricity transfer orbits, Acta Astronautica. 147 (2018) 383-392.

[25] H. Lu, H. Yang, C. Wang, A. Li, Nonlinear deformation and attitude control for spinning electrodynamic tether systems during spin-up stage, Nonlinear Dynamics. 112 (2024) 7011-7027.

[26] H. Lu, C. Wang, A. Li, Y. Zabolotnov, Y. Guo, Sliding Mode Control Strategy of Spinning Electrodynamic Tether Formation During its Spin-up Process, IEEE Transactions on Aerospace and Electronic Systems. 60(1) (2023) 449-462.

[27] B. Yu, K. Ji, Z. Wei, D. Jin, In-plane global dynamics and ground experiment of a linear tethered formation with three satellites, Nonlinear Dynamics. 108(4) (2022) 3247-3278.

[28] C. Du, Z. Zhu, G. Li. Rigid-flexible coupling effect on attitude dynamics of electric solar wind sail. Communications in Nonlinear Science and Numerical Simulation, 95 (2021) 105663.

[29] W. Shen, P. Zhang, Z. Shen, R. Xu, X. Sun, M. Ashry, A. Ruby, W. Xu, K. Wu, Y. Wu, A. Ning, L. Wang, L. Li, C. Cai. Testing gravitational redshift based on microwave frequency links onboard the China Space Station, Physical Review D. 108(6) (2023) 064031.

Thanks For Your Attention

Yang Hang

2024/6/2